

Microstructure and Mechanical Properties of ADI Depending on Austenitization Methods and Parameters

T. Giętka*, T. Szykowny

Department of Materials Science and Engineering, Mechanical Engineering Faculty,
University of Technology and Life Sciences, al. Prof. S. Kaliskiego 7, 85-796 Bydgoszcz, Poland

*Corresponding author. E-mail address: tgietka@utp.edu.pl

Received 22-05-2012; accepted in revised form 31-05-2012

Abstract

Ductile iron was quenched using two-variant isothermal transformation. The first treatment variant consisted of one-phase austenitization at a temperature $t_f = 830, 860$ or 900°C , cooling down to an isothermal transformation temperature of 300 or 400°C and holding from 8 to 64 minutes. The second treatment variant consisted of two-phase austenitization. Cast iron was austenitized at a temperature $t_f = 950^\circ\text{C}$ and cooled down to a supercritical temperature $t_c = 900, 860$ or 830°C . Isothermal transformation was conducted under the same conditions as those applied to the first variant. Ferrite cast iron was quenched isothermally. Basic strength ($R_{p0.2}, R_m$) and plastic (A_5) properties as well as matrix microstructure and hardness were examined.

As a result of heat treatment, the following ADI grades were obtained: EN-GJS-800-8, EN-GJS-1200-2 and EN-GJS-1400-1 in accordance with PN-EN 1564:2000 having plasticity of $1.5\div 4$ times more than minimum requirements specified in the standard.

Keywords: ADI, Austenitizing, Isothermal Process, Mechanical Properties

1. Introduction

ADI castings fabrication involves quenching process using isothermal transformation (usually within a range of $250\text{-}400^\circ\text{C}$) in order to obtain high-carbon austenite and carbon-oversaturated ferrite in the matrix. Such microstructure composition is called ausferrite and the process of isothermal transformation of overcooled austenite – ausferritization [1-6].

During cast iron quenching, the austenitization process, consisting of applying a temperature higher than Ac_1 , should enrich austenite with carbon to the limit marked with the E'S' line and make the metal matrix more uniform. During austenitization of cast iron with initial ferritic microstructure to obtain austenite, only carbon atoms originating from graphite releases are diffused.

The work describes the process of austenitization of a metal matrix and the role of graphite in its carburization [7].

Austenitization occurs usually within temperatures of $815\text{-}950^\circ\text{C}$. The effect of cast iron austenitization depends on chemical composition, initial structure, nodular graphite dispersion, heating temperature and time as well as on the uniformity of elements arrangement in eutectic grains and the size of matrix grains.

A classic method for cast iron austenitization prior to isothermal transformation is one-phase austenitization [1-13].

This work compares selected mechanical properties for one-phase austenitization (classic) at a temperature of $830, 860$ or 900°C or two-phase austenitization. The two-phase variant involved austenitization at a temperature of 950°C and cooling down to a supercritical temperature of $830, 860$ or 900°C . The

assumed supercritical temperatures are identical to austenitization temperatures in the one-phase variant. Isothermal transformation conditions for both austenitization variants were identical: temperature of isothermal transformation – 300 or 400°C with a holding time of 8 to 64 minutes. It was expected when choosing the two-phase austenitization variant that better mechanical properties would be obtained compared to one-phase austenitization. The first austenitization phase should contribute to better matrix uniformity with cooling down reducing carbon concentration in austenite. Smaller carbon content in initial austenite contributes to improvement of plastic properties [3].

2. Material, program and research methods

Ductile iron was smelted in an industrial hot-blast cupola with acid lining. Cast iron spheroidization was conducted in the cupola container using the wire method and ML5 magnesium alloy. Ferrosilicon was used in the modification process. Cast iron was founded into damp sand moulds. Castings had the shape of YII ingots in accordance with PN-EN 1563:2000. Based on the static tensile test, cast iron was classified as EN-GJS-500-7 grade. Cast iron matrix had a ferritic-pearlitic structure (10% pearlite) and graphite had a correct ball-like form. Graphite volume fraction was 11.5% and the amount of releases was 112 per mm² of the microsection surface.

Chemical composition and properties of ductile cast iron are given in Table 1.

Table 1.
The chemical composition and mechanical properties in ductile iron

Chemical element, % mas.					
C	Si	Mn	P	S	Mg
3.65	2.59	0.18	0.052	0.014	0.06
Mechanical properties					
R _m , MPa	A ₅ , %	H, HV10	KCG ₂ , J/cm ²		
507	12.1	156	106		

To obtain a matrix that is fully ferritic, lower parts of an ingot YII were annealed ferritically in a two-phase manner. Then ingots were cut into three flat bars. Flat bars cut from the ingot were marked in accordance with their positioning and five standardised strength test pieces with a gauge diameter of 10 mm were made.

The strength test pieces were quenched applying isothermal transformation in accordance with diagrams provided in Figure 1 and 2. For each treatment, measurements of mechanical properties were carried out for three test pieces originating from one ingot YII. Austenitization was conducted in a chamber furnace and ausferritization in a salt-bath furnace SO140.

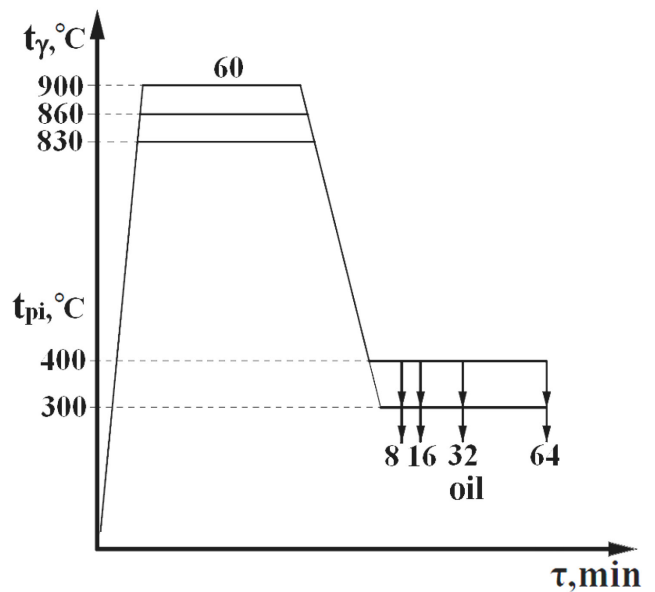


Fig. 1. Scheme depicting austempering of the cast iron according to variant I

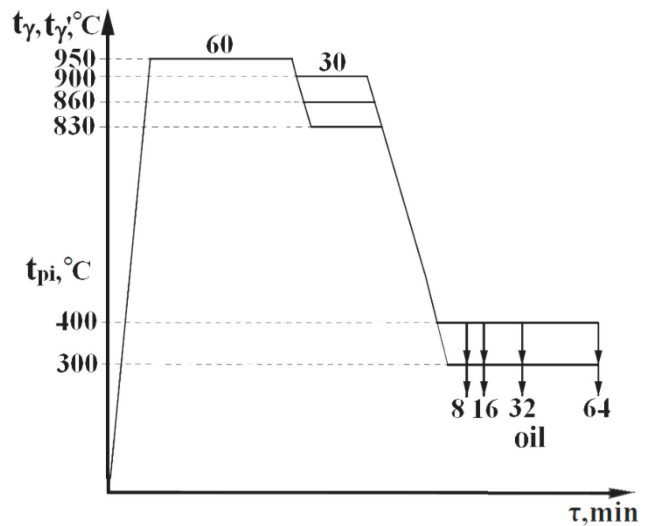


Fig. 2. Scheme depicting austempering of the cast iron according to variant II

Static tensile test was carried out using the testing machine INSTRON type 8502. The tests were aimed to determine tensile strength R_m, proof stress R_{p0.2} and unit elongation A₅.

To assess microstructure, metallographic microsections were made from the gripping part of thermally treated strength test pieces. Inspection and image recording were conducted using a SEM scanning microscope.

Hardness measurements were made on the microsection surface using Vickers method applying a load of 294N. Vickers hardness was converted using comparative tables (PN-93/H-04357) into hardness in Brinell units.

3. The results of the research and their analysis

Hardness in isothermal cooling time function at a temperature $t_{pi} = 300$ and 400°C for variant I and II is presented in Table 2.

Table 2.
The results of hardness measurements

Austenitizing temperature $t_\gamma^1, t_\gamma^2, ^\circ\text{C}$	Isothermal transformation temperature $t_{pi}, ^\circ\text{C}$	Variant of heat treatment	Isothermal transformation time τ_{pi}, min			
			8	16	32	64
			Hardness, HB			
830	300	I	160	170	161	163
		II	388	377	360	386
	400	I	158	161	156	152
		II	249	251	258	248
860	300	I	172	222	151	155
		II	385	381	372	388
	400	I	211	210	195	199
		II	251	254	253	255
900	300	I	402	407	376	396
		II	387	382	369	382
	400	I	251	261	259	258
		II	260	258	261	269

¹⁾ t_γ - austenitization temperature in variant I

²⁾ t_γ - second-phase austenitization temperature in variant II

Tensile strength in isothermal cooling time function at a temperature $t_{pi} = 300$ and 400°C for variant I and II is presented in Table 3.

Table 3.
The results of measurements of tensile strength

Austenitizing temperature $t_\gamma^1, t_\gamma^2, ^\circ\text{C}$	Isothermal transformation temperature $t_{pi}, ^\circ\text{C}$	Variant of heat treatment	Isothermal transformation time τ_{pi}, min			
			8	16	32	64
			Tensile strength R_m, MPa			
830	300	I	473	613	468	453
		II	1422	1395	1385	1425
	400	I	450	455	448	534
		II	956	957	974	976
860	300	I	655	998	545	642
		II	1416	1437	1411	1419
	400	I	760	841	805	855
		II	953	955	956	980
900	300	I	1408	1435	1443	1462
		II	1340	1379	1368	1384
	400	I	957	970	984	947
		II	929	943	964	977

Proof stress in isothermal cooling time function at a temperature $t_{pi} = 300$ and 400°C for variant I and II is presented in Table 4.

Table 4.
The results of measurements proof strength

Austenitizing temperature $t_\gamma^1, t_\gamma^2, ^\circ\text{C}$	Isothermal transformation temperature $t_{pi}, ^\circ\text{C}$	Variant of heat treatment	Isothermal transformation time τ_{pi}, min			
			8	16	32	64
			Proof strength $R_{p0.2}, \text{MPa}$			
830	300	I	316	391	317	315
		II	921	1077	1138	1118
	400	I	320	313	302	372
		II	739	748	765	756
860	300	I	391	696	352	426
		II	883	1047	1133	1134
	400	I	517	601	561	613
		II	703	729	730	745
900	300	I	804	910	1030	1146
		II	787	964	1059	1141
	400	I	625	677	711	717
		II	654	676	694	714

Unit elongation A_5 in isothermal cooling time function at a temperature $t_{pi} = 300$ and 400°C for variant I and II is presented in Table 5.

Table 5.
The results of measurements of relative elongation

Austenitizing temperature $t_\gamma^1, t_\gamma^2, ^\circ\text{C}$	Isothermal transformation temperature $t_{pi}, ^\circ\text{C}$	Variant of heat treatment	Isothermal transformation time τ_{pi}, min			
			8	16	32	64
			Relative elongation $A_5, \%$			
830	300	I	10	4	12	14
		II	4	3	3	3
	400	I	14	14	16	5
		II	9	10	10	9
860	300	I	3	2	5	3
		II	4	5	4	4
	400	I	8	11	8	9
		II	10	12	11	11
900	300	I	3	3	4	4
		II	3	4	4	4
	400	I	8	11	13	8
		II	7	10	12	12

Table 2 shows that quenched cast iron using variant I at a temperature $t_\gamma = 900^\circ\text{C}$ and cast iron held isothermally at $t_{pi} = 300$ or 400°C had a hardness corresponding to ausferritic microstructure. Hardness in this case was within a range of $376 \div 407$ HB for $t_{pi} = 300^\circ\text{C}$ and $251 \div 261$ HB for $t_{pi} = 400^\circ\text{C}$. Inspections of the microstructure of cast iron test pieces following heat treatment using variant I demonstrate that austenitization for $t_\gamma = 830^\circ\text{C}$ occurred within a subcritical range, while for

$t_\gamma = 860^\circ\text{C}$ within an intercritical range of eutectoidal transformation. Therefore, as a result of isothermal transformation, both at a temperature 300 and 400°C , a ferritic ($t_\gamma = 830^\circ\text{C}$) or ferritic-ausferritic ($t_\gamma = 860^\circ\text{C}$) matrix was obtained. Sample microstructure of cast iron subjected to heat treatment using variant I is presented in Figure 3.

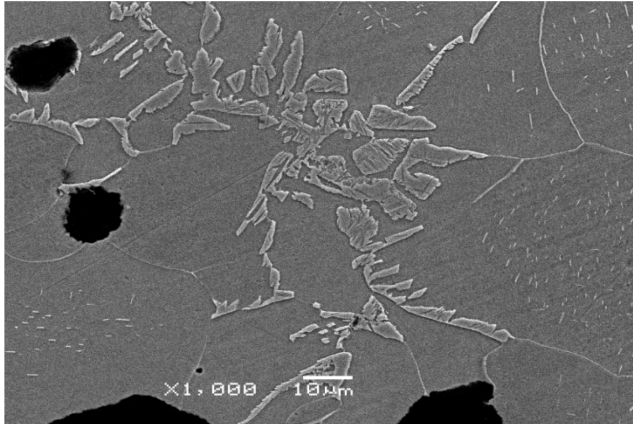


Fig. 3. Microstructure of quenched ductile iron using variant I ($t_\gamma=860^\circ\text{C}$, $t_{pi}=300^\circ\text{C}$, $\tau_{pi}=8$). 1000x magnification, SEM, etched using 2 % alcoholic solution of HNO_3

In variant II of heat treatment, austenite was transformed into lower austenite at a temperature $t_{pi} = 300^\circ\text{C}$. On the other hand, at a temperature $t_{pi} = 400^\circ\text{C}$ austenite changed into upper austenite. This statement is based on hardness test results (Table 2) and microscopic tests. Sample microstructures are presented in Figures 4 and 5.

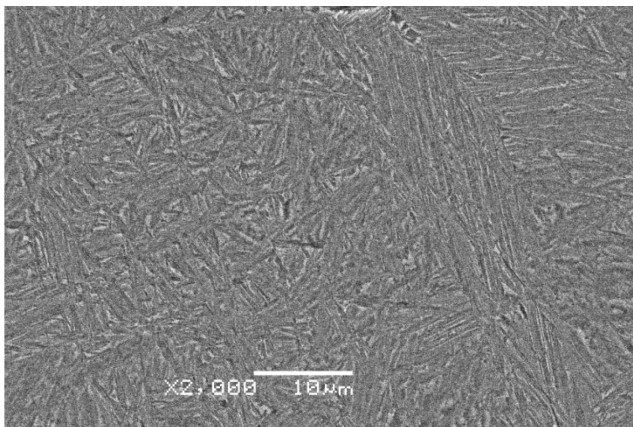


Fig. 4. Microstructure of quenched ductile iron using variant II ($t_\gamma=950^\circ\text{C}$, $t_\gamma=860^\circ\text{C}$, $t_{pi}=300^\circ\text{C}$, $\tau_{pi}=64$). 2000x magnification, SEM, etched using 2% alcoholic solution of HNO_3

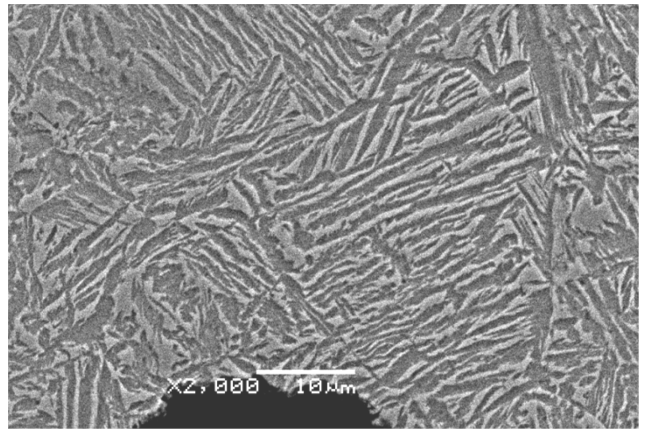


Fig. 5. Microstructure of quenched ductile iron using variant II ($t_\gamma=950^\circ\text{C}$, $t_\gamma=860^\circ\text{C}$, $t_{pi}=400^\circ\text{C}$, $\tau_{pi}=64$). 2000x magnification, SEM, etched using 2% alcoholic solution of HNO_3

Tensile strength (R_m), proof stress ($R_{p0.2}$) and elongation (A_5) in holding time function are presented in tables 3÷5.

Results of tensile tests on test pieces quenched using variant I ($t_\gamma = 830, 860$ and 900°C) at a temperature $t_{pi} = 300^\circ\text{C}$ show that only cast iron quenched from a temperature $t_\gamma = 900^\circ\text{C}$ had microstructure and properties meeting requirements for EN-GJS-1400-1 grade ADI. Austenitization time τ_{pi} had no effect on R_m and A_5 . The results were within a range of $1408\div 1462$ MPa for R_m and $3\div 4\%$ for A_5 . The effect of isothermal quenching time on proof stress $R_{p0.2}$ was significant. With the increase in holding time, up went the value $R_{p0.2}$. The difference in proof stress $\Delta R_{p0.2}$ of ausferritized cast iron within a time from 8 to 64 minutes was 342 MPa (Table 4).

Cast iron quenching using variant I and ausferritization at a temperature $t_{pi} = 400^\circ\text{C}$ allowed parameters corresponding to ADI to be obtained only for the highest temperature $t_\gamma = 900^\circ\text{C}$. Cast iron austenitized at a temperature $t_\gamma = 860^\circ\text{C}$ due to the obtained values R_m , $R_{p0.2}$ and A_5 met requirements for grade EN-GJS-800-8 (except for $\tau_{pi} = 8$ min). The microstructure of this cast iron not only consisted of ausferrite, as required by the definition of ADI, but it also included free ferrite. Ductile iron quenched isothermally within an intercritical range having the structure of free ferrite and ausferrite is marked in literature as FADI [6]. The resulting microstructure corresponding to FADI cast iron is presented in Figure 6.

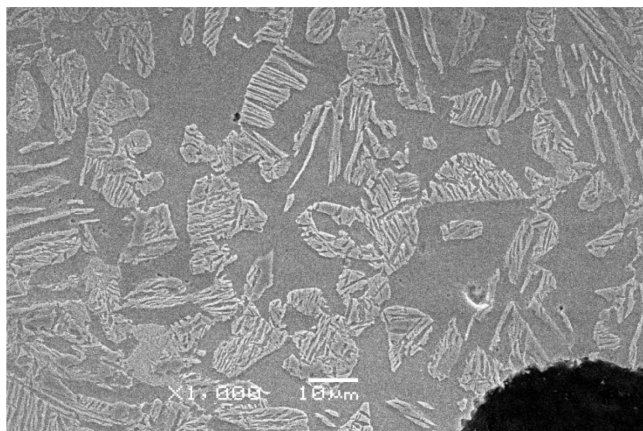


Fig. 6. Microstructure of quenched ductile iron using variant I ($t_\gamma=860^\circ\text{C}$, $t_{pi}=400^\circ\text{C}$, $\tau_{pi}=64$). 1000x magnification, SEM, etched using 2% alcoholic solution of HNO_3

Two-phase austenitization using variant II and ausferritization at $t_{pi} = 300^\circ\text{C}$ resulted in ductile iron having mechanical properties (R_m , $R_{p0.2}$, A_5) corresponding to standardized grades of ADI. Based on the mechanical properties R_m , $R_{p0.2}$ and A_5 , cast iron treated using variant II and ausferritized at $t_{pi} = 400^\circ\text{C}$ was classified as belonging to EN-GJS-800-8 grade. Regardless of the second-phase austenitization temperature, its effect on R_m and A_5 was negligible. On the other hand, proof stress changed depending on the cooling temperature $t_\gamma = 830, 860$ and 900°C : the lower the temperature interval between austenitization and ausferritization, the higher proof stress. As isothermal holding time grew, so grew the values $R_{p0.2}$.

Based on tensile tests and hardness measurements, respective heat treatment variants were ascribed appropriate ADI grades (Table 6).

Table 6. ADI grades classified according to requirements PN-EN 1564 after hardening in accordance with variant I and II

Temp. t_{pi} , $^\circ\text{C}$	Time τ_{pi} , min	Heat treatment					
		Variant I			Variant II		
		830	860	900	830	860	900
400	8	-	-	●	●	●	-
	16	-	-	●	●	●	●
	32	-	-	●	●	●	●
	64	-	-	●	●	●	●
300	8	-	-	◆	◆	◆	■
	16	-	-	◆	■	◆	■
	32	-	-	◆	■	◆	■
	64	-	-	◆	◆	◆	■

● - kind EN – GJS–800–8, ✕ - kind EN–GJS–1000–5
 ■ - kind EN–GJS–1200–2, ◆ - kind EN–GJS–1400–1

Table 6 shows that, notwithstanding the variant, only EN-GJS 800-8 grade was obtained at an isothermal transformation temperature of 400°C . Following ausferritization at a temperature of 300°C , ADI EN-GJS 1400-1 grade was obtained

for variant I and EN-GJS 1400-1, EN-GJS 1200-2 grades for variant II.

In the case of variant I, ADI was obtained only after austenitization at a temperature of 900°C , while for variant II at each second-phase austenitization temperature.

The relation between ausferritization time and hardness, tensile strength and elongation was on the whole insignificant. Specific ADI grade was usually obtained already after the shortest ausferritization time (Table 6). Ausferritization time extension does not lead in the majority of cases to changes in ADI grade. To reduce costs and energy consumption, ausferritization could be finished in most cases after 8 minutes of isothermal holding. After this time, no martensite is observed any longer in cast iron structure. However, due to the continuous and significant increase in proof stress, it is advisable to extend ausferritization time. The relation $R_{p0.2}/R_m$ increases considerably (from 0.59 to 0.82) with the unit elongation value remaining virtually the same. Proof stress is a basic material indicator used in strength calculations. The dependence of $R_{p0.2}$ on time has a degressive nature. As demonstrated by tests, an optimal ausferritization time is around one minute.

4. Conclusion

Based on test results and their analysis, the following conclusions were reached:

1. Heat treatment of ductile iron using variant I allowed ADI to be obtained only after austenitization at a temperature $t_\gamma = 900^\circ\text{C}$. After austenitization at this temperature, ADI with lower ausferrite had strength and plasticity corresponding to EN-GJS-1400-1 grade, while that with upper ausferrite to EN-GJS-800-8.
2. Ductile iron treated using variant II had strength and plasticity corresponding to the following ADI grades: EN-GJS-800-8, EN-GJS-1200-2 and EN-GJS-1400-1.
3. Ductile iron castings with initial ferritic structure may be used for production of ADI.
4. An increase in ausferritization time contributes to a steady and significant increase of proof stress with tensile strength and unit elongation remaining virtually at the same level. The relation $R_{p0.2}/R_m$ is increased within a range of 0.59 to 0.82.

Ausferritization time ensuring optimum combination of ADI strength and plastic properties is around one hour.

References

- [1] Pietrowski S. (1997). Nodular cast iron of bainitic ferrite structure with austenite or bainitic structure. *Archives of Materials Science*. 18 (4), 253-273 (in Polish).
- [2] Guzik S.E. (2003). Austempered cast iron as a modern constructional material. *Inżynieria Materiałowa*. 6, 677-680 (in Polish).
- [3] Dymski S. (1999). *Formation of the microstructure and the mechanical properties of ductile cast iron during isothermal*

- bainitic transformation*. Dissertations no. 95, Section of publishing houses ATR Bydgoszcz, (in Polish).
- [4] Kovacs B.V. (1994). On the Terminology and Structure of ADI. *AFS Transactions*. 102, 417-420.
- [5] Dymski S., Ławrynowicz Z., Giętka T. (2006). Impact strength of ADI. *Archives of Foundry*. 6 (21), 369-376.
- [6] Kilicli V., Erdogan M. (2008). The Strain-Hardening Behavior of Partially Austenitized and the Austempered Ductile Irons with Dual Matrix Structures. *Journal of materials Engineering and Performance*. 17 (2), 240-249.
- [7] Delia M., Alaalam M., Grech M. (1998). Effect of Austenitizing Conditions on the Impact Properties of an Alloyed Austempered. *Ductile Iron of Initially Ferritic Matrix Structure*. 7 (2), 265-272.
- [8] Grech M., Young J.M. (1990). Effect of austenitising temperature on tensile properties of Cu-Ni austempered ductile iron. *Materials Science and Technology*. 6, 415-421.
- [9] Mallia J., Grech M. (1997). Effect of silicon content on impact properties of austempered ductile iron. *Materials Science and Technology*. 13, 408-414.
- [10] Ogi K., Sawamoto A., Jin Y.C., Loper Jr. C.R. (1988). A study of Some Aspects of the Austenitization Process of Spheroidal Graphite Cast Iron. *AFS Transactions*. 96, 75-81.
- [11] Aranzabal J., Gutierrez I., Rodriguez-Ibabe J.M., Urcola J.J. (1997). Influence of the Amount and Morphology of Retained Austenite on the Mechanical Properties of an Austempered Ductile Iron. *Metallurgical and Materials Transactions*. 28A, 1143-1156.
- [12] Eric O. et al. (2006). The austempering study of alloyed ductile iron. *Materials* [DOI:10.1016/j.mat.2006.11.022](#).
- [13] Chang L.C. (1998). Carbon content of austenite in austempered ductile iron. *Scripta Materialia*. 39 (1), 35-38.
- [14] Ławrynowicz Z., Dymski S. (2006). Mechanism of bainite transformation in ductile iron ADI. *Archives of Foundry Engineering*. 6 (19), 171-176.
- [15] Szykowny T. (2005). Isothermal eutectoidal transformation in ductile cast iron EN-GJS-500-7. *Archives of Foundry*. 5 (17), 303-312.
- [16] Dymski S., Giętka T. (2008). Influence of gradual austenitizing on chosen properties of ADI. *Archives of Foundry Engineering*. 8 (3), 185-190.
- [17] Giętka T., Dymski S. (2009). Predicting ADI mechanical properties. *Archives of Foundry Engineering*. 9 (3), 267-274.